VORONOI DIAGRAM AND ITS APPLICATION TO SPATIAL CALIBRATION FOR GAMMA CAMERA IMAGES

Brian D. Maisler, Hong Liu, J. E. McKisson, Yishi Li and Eric Kvam

Embry-Riddle Aeronautical University, 600 Clyde Morris Blvd, Daytona Beach, FL, USA

Abstract: Gamma camera images obtained from PSPMT detectors and segmented crystal scintillators to be used for scintimammography are often distorted and blurred. Our software application is used to restore flood-field gamma camera images and map the peak positions of individual charge clusters back to the positions of the corresponding source scintillations. Since the exact position of scintillation in a crystal grain is not controllable due to the randomness of scattering, a region-to-region location map is more statistically sound than a point-to-point position map. Traditionally, an array of rectangles centered at the restored peaks of charge clusters is mapped to an array of crystal grains from which the source scintillations are emitted. We observe that the mapping is essentially a nearest neighborhood problem and innovatively introduce the Voronoi diagram to replace the rectangular array. The natural fit of the Voronoi diagram to the essence of neighborhood problem significantly improves the likelihood of correct mapping. It also makes our mapping method adaptable to apply to crystal plates in other geometric configurations. We implement the computations of Voronoi diagrams via OpenGL. As an empirical software solution, the images restored from raw flood field images illustrate high level uniformity and linearity.

1 INTRODUCTION

In breast scintimammography, a compact detector with high intrinsic spatial resolution and small inactive peripheries can provide improvements in extrinsic spatial resolution, efficiency and contrast for small lesions relative to larger conventional cameras. The detector that is used by the sponsor of this research is comprised of a segmented array of crystals CsI (TI) optically bonded to a grid of Position Sensitive Photomultiplier Tubes (PSPMTs) (Weisenberger, 2003, Smith 2003, Williams 2000). Tested geometries include both circular and rectangular arrays.

The detection mechanism is conventional scintillation, with optical responses spatially confined into regularly spaced "grains" by the intersegment material. Ultraviolet photons pass through the optical bonding material into the PSPMT envelope to strike the photocathode. The released charge is amplified and the resulting charge cloud is collected on a grid of anode elements. The charge collected on the several anode elements in the PSPMT is electrically gathered along rows and columns by a resistive network and presented at charge sensitive analog to digital converters. The resulting conversions present a vector of raw charge distribution data from which the centroid of the charge cloud is determined in two dimensions. This centroid constitutes the raw centroid data available for each event. Data for the calibration is produced by illuminating the segmented crystal with a uniform planar flood-field gamma ray source. Event data are collected and raw centroids are computed.

Raw flood images obtained in the CsI (TI) array system are intrinsically distorted and blurred (Weisenberger, 2003, Smith 2003, Marks 1999). Optical defects and fabrication limitations cause distortions of the photon collection pattern at the photocathode, and electro-optical effects further distort the charge clouds as they are amplified. Our task is to develop a software application that takes raw flood images as calibration inputs (figure 2), identifies blurred peaks of signals, corrects their distorted positions, and finally maps the individual peaks to the source scintillations. Since the exact position of scintillation in a crystal grain is not controllable due to randomness of scattering, a region-to-region location map is more statistically

sound than a point-to-point position map. Traditionally, the output is a map consisting of rectangles centered at repositioned peaks so that each rectangle maps to a grain of the segmented crystal plate. We observe that the mapping is essentially a closest neighborhood problem and innovatively introduce Voronoi diagram to record the position of the source scintillations. Each polygon contains a point corresponding to the peak of the accumulated charge clouds emitted from a particular crystal grain.
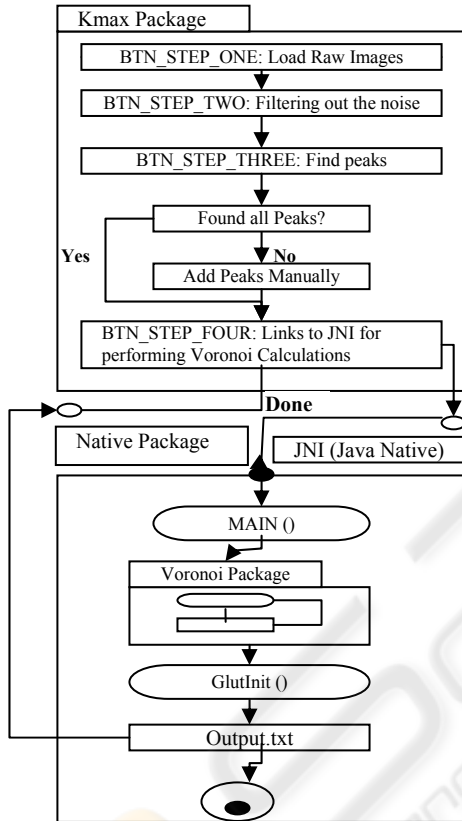
Figure 1.

The application that we developed for image restoration runs under Kmax environment. Kmax is a software product of Sparrow Corp. that provides an environment for creation of Java script files called toolsheets for instrument control and data management with high level support for modular instrumentation, data acquisition, and data analysis (please follow link, http://www.sparrow.com). Our application software consists of two packages. One is a Kmax toolsheet program that interfaces to the end users through routines associated with graphical user interface "buttons" as shown at the top of figure 1. The second package, the block diagram of which is shown at the bottom of figure 1 is a native C

program running in the background. This background task is built on OpenGL to take advantage of graphical tools therein. The two packages are interfaced through Java Native Interface (JNI) functions as shown in Figure 1.

The rest of this article is organized as follows. Section 2 describes our software solution to the image restoration problem. Section 3 focuses on our core geometric technique. We introduce the concept of Voronoi diagram and address the rationale to do so. Section 4 presents our preliminary work on regression methods and an adaptive algorithm for future work.

2 SOFTWARE

This section, we will describe our software solution to the problem introduced above. We present our solution by following the four steps illustrated in the Kmax package of Figure1. In the first step, the raw data file of an image (as shown in figure 2) is loaded and the program is initialized. We outline the other three steps in the following three subsections.

2.1 Filtering Out the Noise

The second step filters noise and enhances peak localization. The filter contains a curve that is roughly the same size and shape as the peaks in the image. The filter is then moved across the image, multiplying the filter by the image beneath it - essentially a correlation function. This process sharpens the image. Figure 3 shows the peak enhanced image.
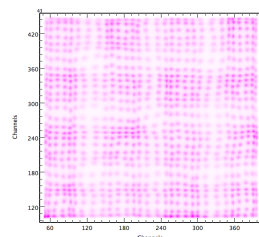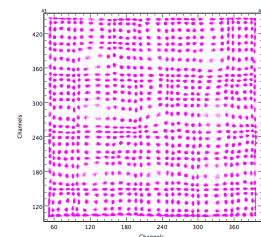
Figure 2: Input Image.   Figure 3: Peak Enhanced Image.

2.2 Find Peaks

The third step is to locate the peaks in the image. We call the set of signals that are emitted from individual source scintillation as a signal cluster. A peak is the centroid of a cluster. Using the filtered

image, a search algorithm attempts to find as many peaks as possible by looking for all local maxima about a user-selected cutoff point.
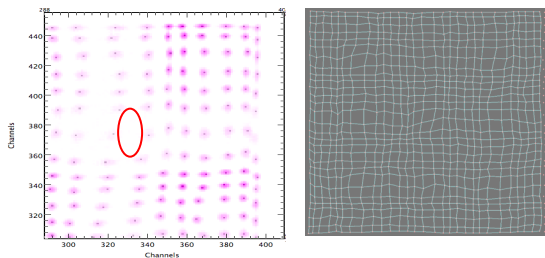

Figure 4: Missed peaks.   Figure 5: Axis warped to peaks.

The search is initiated from the peak closest to the center of the image assuring the peak search works equally well for rectangular and circular detectors. A search ray is projected from the center, initially along the x-axis. The search algorithm iterates finding peaks that are near the axis. The program finds all peaks that are contained within constraints and assigns them a score based on their distance from the center peak and the angle from the search ray. The higher the score, the more likely it is that the peak is the next correct peak on the axis. Significantly higher scoring peaks inside the cone are added to the axis, selecting the smaller angular deviation from the similar scores. The process continues until no peaks fit the constraints, usually when the edge of the image has been reached. The process is repeated for the next row, constructing a new search ray parallel to the next row position until all rows have been registered.

The program will usually find almost all of the peaks, but tends to have trouble near the edges where the image becomes strongly distorted due to the boundaries of crystals and associated losses (see figure 4). Additional problems arise when the calibration image data contain response inhomogeneities, resulting in additional false positive peaks. As shown in the third step of figure one, the located peaks with editing tools are then presented for users to edit them in case some peaks are missing. This is the only step in our current version that requires user interaction. An adaptive algorithm and future work to replace the manual interaction will be presented in section 4.

2.3 Line up Peaks and Built Output File

Once all of the peaks have been identified, all peaks must be horizontally and vertically aligned so that

the calibration file for image restoration can then be built. The program can also find the dimensions of the crystal array by looking at the number of peaks that make up each axis (Figure 5). Once the axes are formed, the last step is to align the rest of the peaks. Since we know that topology of the crystal grains in advance, it is easy to adjust the peak line-up algorithm to work for both rectangular and circular detectors.
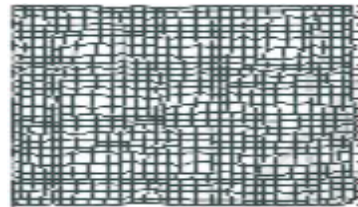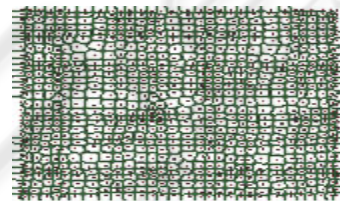

Figure 6: Grids centered at peaks.

Figure 7: Voronoi diagram of the peaks.

Our first mapping file was built on traditional method. As shown in Figure 6, each box centered at a peak maps to a crystal grain from which the charge clouds of the peak are emitted. As shown in the fourth step of figure 1, the mapping file of our current solution was built on Voronoi diagram, which will be elaborated in next section.

3 VORONOI DIAGRAM

This section focuses on our core geometric technique, which is using Voronoi diagram to replace the array of rectangles of the output mapping file. We introduce the concept of Voronoi diagram, outline its implementation, and address the rationale and advantages to introduce this concept to our program.

3.1 Definition of Voronoi Diagram

A Voronoi diagram creates a polygon around each peak such that any point contained within that polygon is closer to that peak than any other peak. This means that when an event is detected, it is mapped to the closest possible crystal. The Voronoi diagram guarantees that every point in a give peak's

polygon is closer to that peak than any other. The Voronoi diagram is built simply by providing a list of points; it is independent of the geometric configuration that the points belong to. In short, it only depends on the peaks that we found.

The Voronoi diagram is one of the most important computational geometry concepts, which is secondary only to convex hulls (O' Rourke, J., 1998). Let $P = \{P_1, P_2, ... P_n\}$ be a set of n points in plane, the nearest neighborhood of P_i is defined as: $V_{P_i} = \{x :| p_i - x | \le | p_j - x |, \forall j \ne i\}$. It is a polygon that contains all points that are closer to p_i than any other points p_j in the point set P. The Voronoi diagram is made up of all neighborhoods V_{P_i} for $1 \le i \le n$.

3.2   Computation of Voronoi Diagram

An efficient algorithm to create Voronoi diagrams as well as its dual Delaunay triangles can be found in the book of O' Rourke. Although our user interface is in Java script, there are two factors that motivate us to code the Voronoi computation in C. Firstly, coding the algorithm in Java reduced the performance measurably. Secondly, OpenGL is coded in C and we would like to build our computation on OpenGL, which provides rich graphic utility functions for us to interpret data and process the graphics elements. The detail implementation is beyond the scope of this article. Source codes are available by personal contact to liuho@erau.edu. Our technical challenge is the interfacing problem with many file operations. We use JNI to interface the Java script code in Kmax and native C codes.

Once the Voronoi diagram is built, the calibration file is created by assigning each crystal element an integer value. This value will represent the array position of the regular crystal that the event will be mapped to. The numbering system starts at the bottom left corner of the array, which is assigned the value of 0 with indices increasing in row order. Event centroids are resolved to an initial pixel position in the raw image. Each pixel in the image space is tested to determine which Voronoi polygon it falls inside and thus which crystal grain the event is to be associated with. The pixel is then assigned the value of the corresponding array position. Once the map has been completed, it is exported in Kmax histogram format. The resulting calibration file is then used to interpret the data when the detector

receives a gamma event. The calibration function takes the apparent (distorted) location of the event and returns the crystal number (position) in which the event is most likely to have occurred.

3.3   The Rationale of Voronoi Approach

We address the rationale to replace rectangular grids to Voronoi diagrams by the deficiency of the former approach and the advantages of the latter one.

Building a *rectangular* array to match the array of crystals presents a number of problems. First, not all of the detectors are rectangular; some detectors are made into circles by cutting off the corners of the crystal array. Second, due to the distortions, especially near the edges, it is difficult to detect exactly where in the array a particular peak belongs. Third, the size of the crystals and the number of crystals changes from detector to detector. It is challenging to make an algorithm that will align the peaks correctly for different geometric configurations of segmented crystal plates.

We know from 3.1 that Voronoi diagram is a geometric concept to describe vicinity. We argue that the mapping between the peaks of signal clusters and the crystal grains is essentially a map between two sets of closest neighborhoods. A PSPMT diagram of the set-up for mapping the detector surfaces with gamma rays can be found in the article by Weisenberger et al. 2003. The charges scattered from the scintillation hit mostly the nearby anode elements within a cylindrical cone whose vertex is the scintillation origin. Notice that the vertical distance from all anodes to the crystal plate are uniform, so, the source scintillation of a charge cluster is most likely originated from the scintillation whose horizontal distance to the peak (centroid of the cluster) is smallest. Since we cannot control the exact location of the scintillation inside a particular crystal grain due to the randomness of scattering, a point-to-point mapping between the scintillation location and their corresponding peaks is not available. Nevertheless, it is statistically sound to assume that most of scintillations originated near the center of the crystal grains. Therefore, the crystal grains that host the corresponding scintillations are their natural nearest neighborhoods in statistical sense. On the other hand, the Voronoi diagrams are the precise nearest neighborhoods of signal peaks. Hence, we have a map between the two sets of neighborhoods; with one set as the nearest neighborhoods of the signal peaks and the other set as the crystal grains that are the natural

neighborhood of the original scintillation.

To summarize the idea: 1. A set of regularly spaced crystal segment grains possess a one to one relationship to peaks identified in the calibration image. 2. The Voronoi diagram of the peak locations define the nearest neighbor mapping from image pixels to the crystal grains (see figure 7). 3. Each imaging event in the scintillator produce a cluster of charge signals at the PSPMT anodes whose centroid falls inside one Voronoi region. 4. The mapping of this centroid from the Voronoi region to the crystal grain defines the shortest distance to the mapped peak among all peaks in the calibration file. 5. Since statistically, most scattering charges of a scintillation hit nearby locations on the detector, the detected cluster of signals is most likely to have originated from a scintillation occurring in the mapped crystal grain corresponding to the containing Voronoi site. Thus, the region-to-region mapping between the two sets of nearest neighborhoods is the best one that is available and necessary in theory. In practice, we can clearly see the differences of linearity and uniformity between the solution in Voronoi diagram approach and the solution in rectangular grids (comparing figure 7 and figure 6). It is desirable to measure the quantitative improvement of in our future work.

The Voronoi diagram will always create a precise nearest neighbor map regardless of geometry. This makes the mapping technique adaptable to crystal plates of other geometric configurations. It is superior to previous methods which defined arbitrary neighborhoods based on a simpler set of bisectors and thus did not guarantee true nearest neighbor performance. The computational complexity of the algorithm for generating the Voronoi diagram $O(n\ ln(n))$, where n is the number of the sites and $ln(n)$ is the natural logarithmic function of vertex number n. It is fast enough for use in real time applications.

4 FUTURE WORK

The third step sometimes relies on manually cropping to correct possible missing peaks, which mostly occurs at edges. Due to the optical and electronic faults, it is possible to incorrectly identify high noises as peaks and falsely filter out low peaks as noises. With judicious choices by the operator the initial peak identification process typically detects 90% to 95% of the true peaks. Our future work is to apply a preliminary nonlinear regression method and an adaptive algorithm presented below to improve

the accuracy of our peak identification.

4.1 Nonlinear Regression

MATLAB is used to implement the nonlinear regression analysis presented below. We try to preprocess the input data file and correct the local distribution of the individual signal clusters without change their total energy levels. The two assumptions are that each cluster observes a hypothetic Gaussian distribution and corresponds to a peak and the distortion does not significantly change the total received energy of a cluster. In our analysis, we first use the local maximum as a reference point to estimate the amplitude of the Gaussian distribution. By substituting the reference point to the model that we have obtained with both the mean and the standard deviation, we can solve for the potential amplitude from the selected reference point. The second step is to identify those significantly distorted data by calculating the difference between the experimental data and the predicted data. The third step is to correct them in the direction of the estimated trend by keeping the mean invariant according to the second assumption. After constructing the Gaussian distribution the deficient data values are replaced by the values suggested by the regression curve. This procedure is performed iteratively until the difference between the interactions is sufficiently small (see Figure 8).

4.2 An Adaptive Algorithm

We need firstly to set the criteria to measure the quality of our calibration. Regardless whether we use rectangular crystal plate or round crystal plate, we know the numbers of the crystal grains in each row and each column. We also recall that our Voronoi diagram has been indexed horizontally and vertically at the fourth step. So our first measure is that the numbers of sites in each row and each column of Voronoi diagram must match those of the crystal plate. We also know that the sizes of crystal grains are almost uniform except for the grains on the edge of round crystal plates. Though distortion is inevitable, we expect that the Voronoi diagram has a certain level of uniformity of sizes, which is measured by the number of pixels. Hence, our second measure is the statistical confidence level of the site sizes. We define our fitness function of the adaptive algorithm according to these two factors with empirical weighted coefficients.

In the first step of iteration, the image data modified in the previous iteration is loaded to

replace the raw data. Our major change starts at the third step as follows: We mark those narrowly passed peaks as likely false peaks. While those points passing a specific cutoff filter are recorded as peaks, other points passing half of the cutoff filter or whose amplitudes being second to the corresponding peaks nearby are also recorded as back-up candidate peaks for next iteration. They are used to mutate with the narrowly passed peaks to improve the overall fitness function in the fourth step.
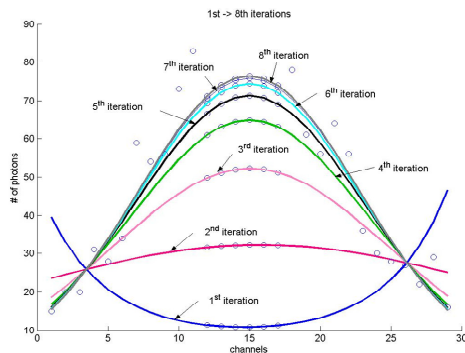

Figure 8: Nonlinear Regressions of Several Iterations.

After constructing the Voronoi diagram and indexing each site with the mapped pixels, we add three operations in the fourth step. Firstly, we recalculate the median and standard variations of the site sizes along with the amplitude of signals and update the fitness function. Secondly, we construct a hypothetic Gaussian distribution of the site sizes of the Voronoi diagram. If the size of a peak lies out of the small side of a certain confidence interval, then it is confirmed as a most-likely false peak. If a recorded back-up peak candidate is available in the corresponding site of the most-likely false peak, then, we test the mutation under the fitness function. If the mutation improves the fitness, then the back-up point is promoted as a peak by properly increasing its signal amplitude without changing the mean signal intensity, while the most likely false peak is demoted as a back-up candidate by properly decreasing its amplitude. Finally, we use an empirical cutoff of the fitness function to decide if the iteration should be terminated.

4.3 Conclusions

Voronoi diagram has extensive applications in many fields (Gonzalez 2004). In the broad image processing field, Amidror surveyed the applications of Voronoi diagrams to data interpolations Amidror 2002. We observe that the mapping between the peaks of charge clouds and scintillation sources of a segmented crystal plate is essentially a nearest neighborhood problem. In this work, we use a Voronoi diagram to construct the position mapping. To our knowledge, it is the first time that the Voronoi diagram is applied to solve position mapping problems in image processing field. The natural fit of the Voronoi diagram to the essence of neighborhood problem significantly improves the likelihood of correct mapping and makes the mapping technique adaptable to crystal plates in other geometric configurations. This paper presents our empirical solution to the image restoration problem used for breast scintimammography. We implement the computation of Voronoi diagrams in C via OpenGL under a Java-based user environment called Kmax. We also outline a nonlinear regression method to correct the shape of charge clusters locally and a preliminary adaptive algorithm to improve the effectiveness of peak identification in our future work.

ACKNOWLEDGEMENTS

REFERENCE

Amidror, I., 2002. Scattered data interpolation methods for electronic imaging system: A survey, *Journal of Electronic Imaging* , Vol. 11(2), 157-176.

Gonzalez, R., C., Woods, R., E., 2004. *Digit Image Processing,* Pearson Education, *,* 2nd edition.

Weisenberger, A.G., Wojcik, R., et al. 2003. SPECT-CT system for small animal imaging, *Nuclear Science, IEEE Transactions, Volume 50, Issue 1,* pp. 74 – 79.

Marks, D.G., Barber, H.B., et al., 1999. Improving Performance of a CdZnTe imaging array by mapping the detector with gamma rays, *Nuclear Inst. & Methods in Phys. Res.,* A 428, 102 – 112.

O' Rourke, J., 1998. *Computational Geometry in C,* Cambridge University Press, second edition.

Smith, M.F, Majewski, S., Weisenberger, A.G., 2003. Optimizing Pinhole and Parallel Hole Collimation for Scintimammography with Compact Pixellated Detectors, *IEEE Trans Nucl Sci.* 50: 321-326.

Williams, M. B., Goode, A.R., Galbis-Reig, V., et al. 2000. Performance of a PSPMT based detector for scintmammorgraphy, *Phy. Med. Biology*, Vol. 45, pp 781-800.